# Multifunctional Bandpass Filter With Codesigned Tunable Attenuator and Reflectionless Phase Shifter Functionalities

Zixiao Zhang, *Graduate Student Member, IEEE*, and Dimitra Psychogiou, *Senior Member, IEEE*

***Abstract*— A multifunctional bandpass filter (BPF) with two switchable modes of operation, namely: 1) a codesigned reflectionless BPF and variable phase shifter (BPF-VP) with 360° phase shift and 2) a codesigned BPF and variable attenuator (BPF-VA) is reported. The multifunctional BPF can also be intrinsically switched-off when operating in the BPF-VP mode. It is based on a combination of a filtering rat-race coupler (RFRC) with continuously tunable power and a switchable phase coupling element that controls the mode of operation. Notably, the proposed component combines four different functions, namely BPF, VP, VA, and RF switch into a single component, reducing the size of the RF front-end (RFFE). As a proof-of concept, a multilayer prototype was manufactured and tested. It exhibited: 1) a third-order BPF-VP at 700 MHz with a 360° continuously tunable phase and a reflectionless bandwidth of 375 MHz–1.093 GHz; 2) a switching off state with >25 dB of isolation; and 3) a third-order BPF-VA mode at 700 MHz with tunable attenuation between 4 and 25 dB.**

***Index Terms*— Attenuators, bandpass filter (BPF), phase shifters.**

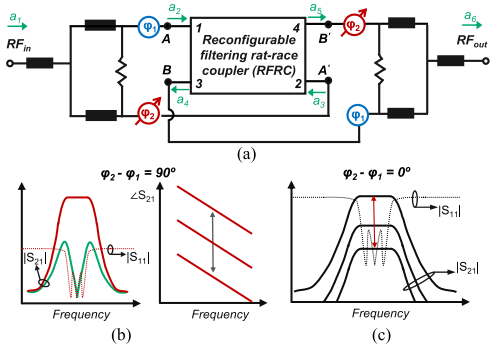


Fig. 1. (a) Block diagram of the multifunctional RF filter that exhibits a BPF-VP and a BPF-VA modes of operation. Reconfigurability between the two modes is obtained by a tunable-phase coupling element. (b) Reflectionless BPF-VP mode of operation when $\varphi_2 - \varphi_1 = 90°$ with a 0°–360° of phase shift by altering the coupling ratio of the RFRC. (c) BPF-VA mode of operation when $\varphi_2 - \varphi_1 = 0°$. A continuously tunable attenuation between 0 and $\infty$ dB can be obtained by altering the coupling ratio of the RFRC.

## I. Introduction

VARIABLE attenuators, phase shifters, and RF filters are indispensable components of practically every phased-antenna array RF system [1]. Driven by the growing demand for multifunctional RF transceivers with low weight, size, and weight (SWaP), there is an increasing interest in integrating multiple functionalities within the volume of a single RF component to reduce the size of the RF front-end (RFFE). A particular emphasis has been given to the development of RF-filter-based codesign techniques that allow the incorporation of RF filtering with other signal processing functions, e.g., attenuation, phase shifting, or RF switching. Typical examples of this trend include variable filtering attenuators (VFAs) [2], [2], [3], [4], [5], and variable filtering phase shifters (VFPSs). Different design methods have been reported for the design of VFAs, however, they encounter the following challenges: 1) restricted attenuation range (under 15 dB) [2], [3], [5]; 2) low selectivity [4]; and 3) compromised return loss and transfer function shape when adjusting their attenuation [2], [3], [4]. Research on VFPS has also been conducted [6], [7], however, existing VFPS are limited to second-order transfer functions and only offer a single filtering mode of operation. Wei et al. [8] introduces variable-amplitude capability in the VFPS, however, it is constrained to a second-order transfer function whose shape changes during the tuning process.

Considering these limitations, this letter introduces for the first time a new multifunctional BPF that combines the function of: 1) a codesigned bandpass filter (BPF) and variable phase shifter (BPF-VP) with a continuously tunable 360° phase shift with reflectionless characteristics as well as switching off capability and 2) a codesigned BPF and variable attenuator (BPF-VA) with a theoretically tunable attenuation between 0 and $\infty$ dB. Furthermore, in both modes of operation, the filtering transfer function is consistently preserved for all tuning states.

## II. Design Principles

The proposed multifunctional filter is shown in Fig. 1. It comprises two power splitting/combining networks, a static phase coupling element $\varphi_1$ (marked in blue), a reconfigurable phase coupling element $\varphi_2$ (marked in red), and a coupled-resonator-based reconfigurable filtering rat-race coupler (RFRC). The input and output networks are connected to the RFRC ports at A, A′ and B, B′, respectively, through $\varphi_1$ and $\varphi_2$. In this manner, by changing the phase of $\varphi_2$, the output phases at A′ and B′ can change between 90° or 0° relative to the phases at A and B, enabling the multifunctional filter to switch between the BPF-VP and the BPF-VA mode as shown in Fig. 1(b) and (c). In what follows, the operating principles of the multifunctional filter are described in detail.

Manuscript received 21 February 2024; accepted 5 March 2024. Date of publication 25 March 2024; date of current version 7 June 2024. This work was supported by the Science Foundation Ireland (SFI) Project under Grant 20/RP/8334. *(Corresponding author: Zixiao Zhang.)*

The authors are with the School of Engineering, University College Cork, Cork, T12 K8AF Ireland, and also with the Tyndall National Institute, Cork, T12 R5CP Ireland (e-mail: zixiao.zhang@tyndall.ie; DPsychogiou@ucc.ie).

This article was presented at the IEEE MTT-S International Microwave Symposium (IMS 2024), Washington, DC, USA, June 16–21, 2024.

Color versions of one or more figures in this letter are available at https://doi.org/10.1109/LMWT.2024.3377266.

Digital Object Identifier 10.1109/LMWT.2024.3377266

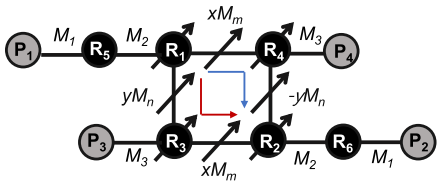


Fig. 2. RFRC exhibiting a third-order BPF response. Gray circles: ports, black circles: static resonators, black circles with an arrow: tunable resonators, black lines: static couplings, black lines with an arrow: tunable couplings.

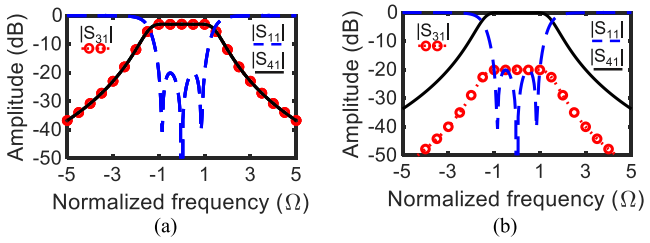


Fig. 3. Synthesized S-parameters of the RFRC when $M_1 = M_3 = 1.0837$, $M_2 = 1.0317$. (a) $k = 1$, $M_m = M_n = 0.7295$. (b) $k = 100$, $M_m = 1.0266$, $M_n = 0.1027$.

### A. Reconfigurable RFRC

The coupling routing diagram of the RFRC is shown in Fig. 2. The four-port network ($P_1$–$P_4$) consists of four tunable resonators $R_1$–$R_4$ and two static resonators $R_5$ and $R_6$, static couplings $M_1$–$M_3$, and reconfigurable mixed couplings $M_m$ and $M_n$. In this context, $x$ and $y$ are utilized to indicate the coupling polarities, which can be selected as either 1 or $-1$. When power is inserted in $P_1$, the signals reaching $R_2$ via two different paths have identical coupling strength but are 180° out of phase, thus $P_2$ is isolated. Consequently, all the power from $P_1$ is distributed to $P_3$ and $P_4$ according to a power division ratio $k$, which is determined by $M_m$ and $M_n$ as: $M_m = \sqrt{k}M_n$.

Fig. 3(a) and (b) demonstrates two synthesized $S$-parameter responses for two different power division ratios $k = 1$ and 100 for a Chebyshev response with 0.0431 dB ripple. When $k = 1$, the power from $P_1$ is equally divided between $P_3$ and $P_4$. When $k = 100$, the power delivered to $P_4$ is 20 dB less than that delivered to $P_3$. It is noted that the third order Chebyshev response is maintained for any $k$.

### B. BPF-Variable Phase Shifter Mode

When $\varphi_2 - \varphi_1 = 90°$ [see Fig. 1(b)], the RF filter operates in the BPF-VP mode and exhibits a 360° continuously tunable phase shift. Its behavior can be analyzed using (1)–(7). Equation (1) lists the incident power waves at $P_1$ and $P_2$ of the RFRC, where $\theta_{pd}$ represents a constant phase delay introduced by the coupling elements. Equation (2) details the scattering matrix ($S_c$) of the RFRC at the center frequency, and (3) addresses the power relationship within the RFRC. Combining (1)–(3), the output power wave $a_4$ can be expressed in relation to $a_1$. Using (4), the overall output power wave of the BPF-VP $a_6$ can be expressed as a function of $a_4$, and consequently in terms of $a_1$, leading to expression (5). Using (5) as a reference, the amplitude $|S_{21}|$ and the phase $\angle S_{21}$ of the power transmission response of entire BPF-VP can be calculated and is listed in (6) and (7). As shown, $|S_{21}|$ is always equal to 1, while the insertion phase varies as a function of $x$, $y$, and $k$ as shown in the conditions in (8)–(11). By adjusting both the polarity and the magnitude of the couplings between $R_1$ and $R_4$, a 360° phase variation can be obtained. Additionally, owing to the 90° phase difference between A and A' (and between B and B'), signals reflected outside of the passband in both paths have equal amplitude but are 180° out of phase. This leads to reflectionless responses at both the RF input and output ports

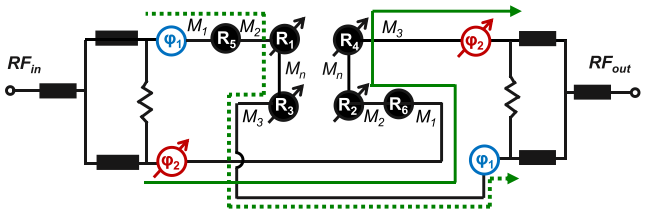


Fig. 4. Signal flow at BPF-VP mode when the $M_m = 0$ making the multifunctional BPF to intrinsically switch-off.

$$a_2 = \frac{a_1}{\sqrt{2}} e^{j\theta_{pd}}, \quad a_3 = a_2 e^{-j\frac{\pi}{2}} \tag{1}$$

$$[S_c] = \frac{-j}{\sqrt{k+1}} \begin{bmatrix} 0 & 0 & y \times 1 & x\sqrt{k} \\ 0 & 0 & x\sqrt{k} & -y \times 1 \\ y \times 1 & x\sqrt{k} & 0 & 0 \\ x\sqrt{k} & -y \times 1 & 0 & 0 \end{bmatrix} \tag{2}$$

$$a_4 = S_{c\_31} a_2 + S_{c\_32} a_3 \tag{3}$$

$$a_6 = \sqrt{2}\, e^{j\theta_{pd}} a_4 \tag{4}$$

$$|a_6| = |a_1|, \angle a_6 = \theta_{pd} + \arctan\left(\frac{-x\sqrt{k} - jy}{\sqrt{k+1}}\right) + \angle a_1 \tag{5}$$

$$|S_{21}| = \frac{|a_6|}{|a_1|} = 1 \tag{6}$$

$$\angle S_{21} = \angle a_6 - \angle a_1 = 2\theta_{pd} + \arctan\left(\frac{-x\sqrt{k} - jy}{\sqrt{k+1}}\right) \tag{7}$$

$$-180° \le \angle S_{21} \le -90°, \quad x = 1, y = 1 \tag{8}$$

$$90° \le \angle S_{21} \le 180°, \quad x = 1, y = -1 \tag{9}$$

$$90° \le \angle S_{21} \le 180°, \quad x = 1, y = -1 \tag{10}$$

$$-90° \le \angle S_{21} \le 0°, \quad x = -1, y = 1. \tag{11}$$

Fig. 4 shows the signal flow diagram for the intrinsically switched-off state of the component. This functionality is achieved by setting $M_m = 0$, while maintaining identical coupling values between $R_1$ and $R_3$, and between $R_2$ and $R_4$. As indicated in Fig. 4, the input power is transmitted to the output port solely via two paths: through $R_5$, $R_1$, $R_3$ (indicated in green dashed line), and through $R_6$, $R_2$, $R_4$ (indicated in green solid line). These paths effectively cancel each other out, as they carry signals of the same amplitude but are 180° out of phase. As a result, the component is intrinsically switched-off.

### C. BPF-Variable Attenuator Mode

When $\varphi_2 = \varphi_1$ as indicated in Fig. 1(c), the device operates in the BPF-VA mode. Its operation can be described by (12)–(15). According to (15), the power transmission response can vary between 0 and 1 when $k$ is varied from 0 to $+\infty$

$$a_2 = a_3 = \frac{a_1}{\sqrt{2}} e^{j\theta_{pd}} \tag{12}$$

$$a_4 = S_{c\_31} a_2 + S_{c\_32} a_3, \quad a_5 = S_{c\_41} a_2 + S_{c\_42} a_3 \tag{13}$$

$$a_6 = \frac{\sqrt{2}}{2} e^{j\theta_{pd}} (a_5 + a_4) \tag{14}$$

$$|S_{21}| = \frac{|a_6|}{|a_1|} = \left|\frac{\sqrt{k}}{\sqrt{k+1}}\right|. \tag{15}$$

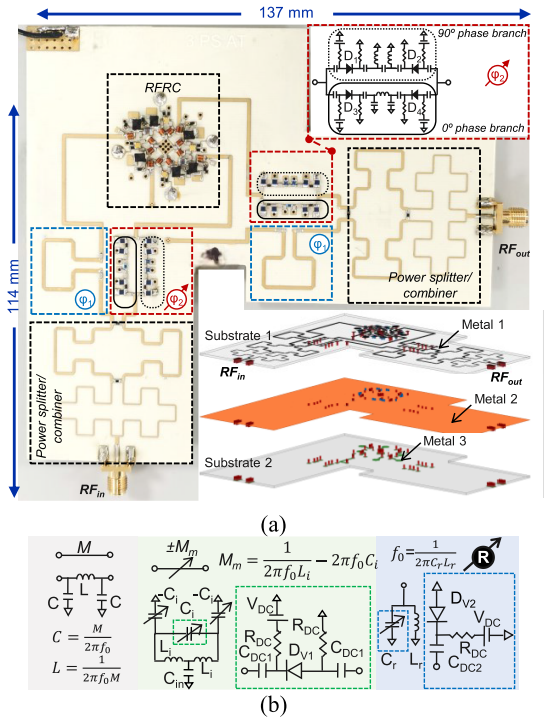


Fig. 5. (a) Top-view of the manufactured prototype, 3-D view of the multilayer PCB integration concept of the multifunctional BPF-VP/BPF-VA. (b) From left to right: static coupling $M$, reconfigurable coupling $M_m$ and frequency tunable resonator.

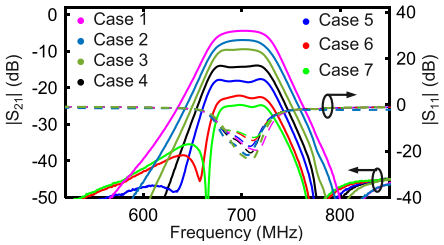


Fig. 6. RF measured S-parameters of the multifunctional filter when operating in the BPF-VA mode for seven tuning cases.

## III. Experimental Validation

The proposed multifunctional BPF-VP/BPF-VA concept has been validated through the EM design, manufacturing, and testing of a multilayer prototype on a Rogers 4003 three-layer stack-up as shown in Fig. 5(a). The prototype was implemented for a center frequency of 700 MHz and a fractional bandwidth of 10%. Multiple layers were used to facilitate the realization of the crossover in Fig. 1. The power splitting/combining networks are constructed using a wide-band Wilkinson-power divider, followed by the static phase coupling elements $\varphi_1$ (shown in blue dash boxes) and tunable phase coupling elements $\varphi_2$ (indicated in red dash boxes) to enable a switchable 0°/90° phase difference output. $\varphi_2$ can be switched between the two branches by controlling four PIN diodes. Specifically, when $D_1$ and $D_2$ are on and $D_3$ and $D_4$ are OFF, $\varphi_2 - \varphi_1 = 90°$, and the component works in the BPF-VP mode. Conversely, when $D_1$ and $D_2$ are OFF while $D_3$ and $D_4$ are ON, an in-phase output is obtained between $\varphi_2$ and $\varphi_1$ and the RF component operates in the BPF-VA mode. Frequency tunable resonators are used to facilitate an almost constant transfer function shape and compensate out the inverter parasitics when tuned by varactors, thus no longer being 90° at the design frequency. They are implemented by tunable $LC$ tanks as in Fig. 5(b). The static couplings are implemented by their first-order low-pass $\pi$-network equivalent while the reconfigurable couplings are implemented by a parallel combination of a high-pass $\pi$-network providing electric coupling and a low-pass $T$-network providing magnetic coupling.

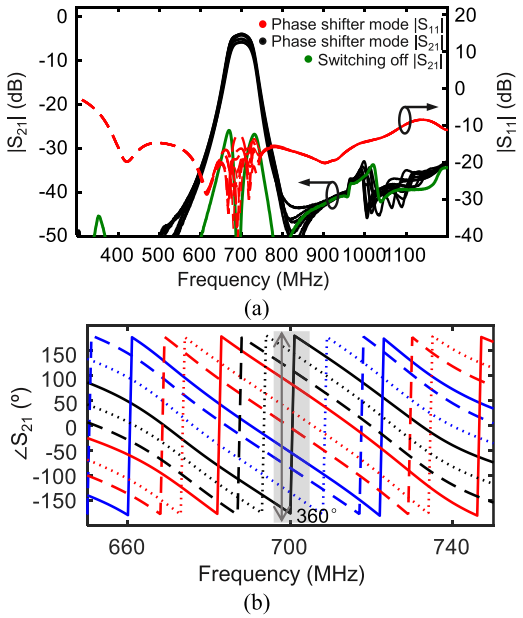


Fig. 7. RF measured S-parameters of the multifunctional filter when operating in the BPF-VP mode. Nine cases are shown. (a) Amplitude responses. (b) Insertion phase tuning responses.

TABLE I
Comparison With State-of-Art Codesigned Filters

| Ref. | Mode | $f_{cen}$(GHz) | TF | PTR (°) | ATR (dB) | RBW (GHz) | Size ($\lambda_g$*$\lambda_g$) | OFF | CTF |
|---|---|---|---|---|---|---|---|---|---|
| This | VP | 0.7 | 3rd | 360 | No | 0.72 | 0.6*0.5 | Yes | Yes |
| | VA | 0.7 | 3rd | No | 15.8 | No | | | |
| [4] | VA | 1.01~1.19 | 2nd | No | 18 | No | N/A | No | No |
| [5] | VA | 2 | 5th | No | 12 | No | 0.64*0.2 | No | Yes |
| [6] | VP | 1.05~1.3 | 2nd | 320 | No | No | 0.9*1.1 | No | No |
| [7] | VP | 0.69 | 2nd | 340 | No | No | 0.3*0.3 | No | Yes |
| [8] | VA+VP | 0.75~0.95 | 2nd | 360 | 10 | No | N/A | No | No |

TF: transfer function, PTR: phase tuning range, ATR: attenuation tuning range, CTF: constant transfer function.

A photograph of the prototype is provided in Fig. 5(a) and its RF measured performance is shown in Figs. 6 and 7 for the BPF-VA and the BPF-VP modes, respectively. Although seven distinct states are shown, the attenuation is continuously tunable between 4.2 and 25 dB at 700 MHz as indicated in Fig. 6. As shown, both the passband shape and the return loss remain almost constant across the entire tuning range. Fig. 7 showcases the measured results of the device when operating in the BPF-VP mode for nine states although it is continuously tunable between among all of these with an overall continuously tunable phase shift of 360°. Also, in this case, a well-preserved passband response is obtained for all tuning states [see Fig. 7(a)] with an insertion loss (IL) between 4 and 6 dB. The finite levels of IL are due to the finite $Q$ of the SMD inductors and varactors. However, it is reasonable given that the proposed component integrates four functionalities at the same time. Additionally, the BPF-VP mode demonstrates a very wide reflectionless BW between 375 and 1093 MHz. By reconfiguring the couplings, an intrinsically switched-off state can also be obtained as exemplified by the green trace in Fig. 7(a). The measured IIP3 varies from 14 to 20 dBm for all the cases.

A comparison of the proposed multifunctional BPF with the state-of-the-art multifunctional RF codesigned filters is provided in Table I. When compared to the VAs in [4] and [5], the proposed topology not only delivers a BPF response of a higher order but also has wider attenuation tuning range and attains an almost constant transfer function. When compared to the VPs in [6] and [7], the proposed concept demonstrates wider tunable phase shift range and an almost constant transfer function. In addition, it has a VA mode and can also be intrinsically switched off. Overall, it is the only multifunctional BPF that combines multiple tunable modes of operation with high levels of flexibility, intrinsic switching off capability and reflectionless transfer function, which can be used to cancel unwanted reflections in the RFFE.

## IV. Conclusion

This work has successfully developed and validated a multifunctional BPF with two operational modes: a BPF-VP and a BPF-VA. The proposed structure integrates four functionalities into a single component, which includes a third-order reflectionless BPF, an attenuator with variable attenuation levels and a phase shifter with continuously phase tuning capability and switching off functionality. The developed prototype at 700 MHz, demonstrated a third-order BPF-VP with 360° phase tuning, a broad reflectionless bandwidth spanning from 375 to 1093 MHz and intrinsic switching off capability, as well as a third-order BPF-VA with a tunable attenuation range of 4–25 dB. Notably, the filtering transfer function is consistently preserved for all tuning states.

## References

[1] D. Zhao et al., "Millimeter-wave integrated phased arrays," *IEEE Trans. Circuits Syst. I, Reg. Papers*, vol. 68, no. 10, pp. 3977–3990, Oct. 2021.

[2] B. Wu et al., "Dynamically tunable filtering attenuator based on graphene integrated microstrip resonators," *IEEE Trans. Microw. Theory Techn.*, vol. 68, no. 12, pp. 5270–5278, Dec. 2020.

[3] J. M. Knowles, H. H. Sigmarsson, and J. W. McDaniel, "Higher-order filtering attenuator design considerations for filter shape optimization," in *Proc. IEEE Wireless Microw. Technol. Conf. (WAMICON)*, Melbourne, FL, USA, Apr. 2023, pp. 85–88.

[4] Z. Wei, S. Chen, X. Zhu, P.-L. Chi, R. Xu, and T. Yang, "Reconfigurable filtering attenuator with continuously tunable center frequency and amplitude," in *IEEE MTT-S Int. Microw. Symp. Dig.*, Denver, CO, USA, Jun. 2022, pp. 187–190.

[5] J. Li, W. He, K.-D. Xu, J. Chen, and X. Y. Zhang, "Compact tunable broadband filtering attenuator based on variable resistors," *IEEE Microw. Wireless Technol. Lett.*, vol. 33, no. 7, pp. 983–986, Jul. 2023.

[6] X. Zhu, T. Yang, P.-L. Chi, and R. Xu, "Novel passive vector-sum reconfigurable filtering phase shifter with continuous phase-control and tunable center frequency," *IEEE Trans. Microw. Theory Techn.*, vol. 70, no. 2, pp. 1188–1197, Feb. 2022.

[7] Z. Zhang and D. Psychogiou, "Non-reciprocal RF co-designed filtering phase shifters with continuously tunable phase shift," in *Proc. 53rd Eur. Microw. Conf. (EuMC)*, Sep. 2023, pp. 102–105.

[8] Z. Wei, X. Chen, X. Zhu, P. Chi, R. Xu, and T. Yang, "Novel passive vector-sum amplitude-variable phase shifter with integrated reconfigurable filtering function," *IEEE Trans. Microw. Theory Techn.*, vol. 70, no. 7, pp. 3511–3523, Jul. 2022.